Measurement and Analysis of Nuclear Heat Depositions in Structural Materials Induced by D-T Neutrons

Y. Ikeda, , C. Konno, K. Kosako, Y. Oyama,
F. Maekawa, H. Maekawa
Japan Atomic Energy Research Institute,
Tokai, Ibaraki 319-11, Japan
Tel. 81-292-82-6016

A. Kumar, M.Z. Youssef, M. A. Abdou

University of California, Los Angeles
Los Angeles, CA 90024, USA
Tel. 1-310-825-8627

ABSTRACT

Nuclear heat deposition rates in ten different materials, Li_2CO_3, Graphite, Ti, Ni, Zr, Nb, Mo, Sn, Pb and W, subjected in D-T neutrons have been measured by a microcalorimetric technique in the frame work of JAERI/USDOE collaborative program on fusion neutronics. A great improvement in accuracy of experimental data was achieved by introducing a high sensitivity voltmeter and applying constant current on the thermal sensors. The measured heating rates were compared with calculations to verify the adequacy of the currently available data base relevant to the nuclear heating process. In general, calculations with data of JENDL-3 and ENDL-85 libraries gave excellent agreements with experiments for all materials except Zr. The calculation with the MBCCS suffered large discrepancy from measurement.

I. INTRODUCTION

Importance of nuclear heating in the structural materials has been recognized from the critical system design of D-T fusion reactors. The accuracy of the data base relevant to the nuclear heating is considered as one of most crucial problems in the designs. Many data libraries have been compiled and issued so far to be implemented in the neutron transport code system.1-6) Adequacy of the data has been tested through the integral experiment as the common course of the data evaluation. An attempt to measure nuclear heating in D-T neutron field was initiated7,8) at the fusion neutronics source facility9). Since 1989, extensive effort has been devoted on the development of measuring technique for the nuclear heating in the D-T fusion environment in the framework of the JAERI/USDOE collaboration on fusion neutronics[10,11]. The microcalorimetric method has been introduced in the measurement. This technique gives direct and totally integrated results associated with the heating process by neutrons in the materials. Although the microcalorimetric method has been applied in the reactor dosimetry studies,[12-16] we had to develop a sophisticated method to measure very small signal for the temperature rise due to nuclear heating, because of limitation in D-T neutron source, strength of which was around 3×10^{12}/s.

The previous papers on this subject have shown the basic experimental procedure and the preliminary results.[10,11] Some improvement has been made on the measuring system in terms of increasing the accuracy of the voltmeter, thermally stabilizing the probes, elimination of the scanner for the output signals. The present study includes new material proves of Li_2CO_3, Zr, Nb, Sn and Pb in addition to the materials already subjected. Some materials of importance, such as graphite and tungsten, were re-examined to give better qualified data and to realize reproducibility of the system. The experimental analysis was carried out by using neutron transport codes and nuclear data libraries. The most important mission of this experimental program is to test the heating data base currently available. Integral test in terms of the C/E (ratio of calculation to experiment) gives direct information for this test.

In this technique, no discrimination of the neutron and gamma-ray contribution is possible since both neutron and associated γ-ray contribute to the heat deposition in the materials. Moreover, radiations from the materials surrounding the probe also contributes to the temperature rise.

II. EXPERIMENTS

2.1. Concept for the nuclear heating measurement

Very small temperature rise due to nuclear heating is expected in materials subjected in neutron flux level from 10^9 to $10^{10}/cm^2/s$, which is considered a limit to generate nuclear heating signal as long as the available neutron source strength at FNS[9] is concerned. The corresponding temperature rise ranging from 10^{-4} to 10^{-5} K/s has been observed in the previous experiments. It is critical to detect such a slight signal against the large background of changes in room temperature. To meet the critical condition, the following are required;

(1) stabilization of the microcalorimeter,
(2) precision of electric device with low noise,
(3) elimination of the background noise.

Even though these conditions are satisfied, there is an inherent heat source due to the current applied on the resistance of the thermal sensor. To eliminate the macroscopic temperature change governed by the current source and ambient temperature change, the slope of temperature change was differentiated by taking derivatives for each subsequent data. This process is depicted in Fig. 1. In this regard, the stability of background drift is very essential to realize a good signal to noise ratio. The static background noise, of course, should be kept to be as low as possible. Before differentiation, direct temperature gave poor signal to noise ratio (S/N) less than 10^{-5}; in room temperature at 25 °C, the slope to be detected could be 10^{-4} K/sec. It is impossible to derive the signal from the direct

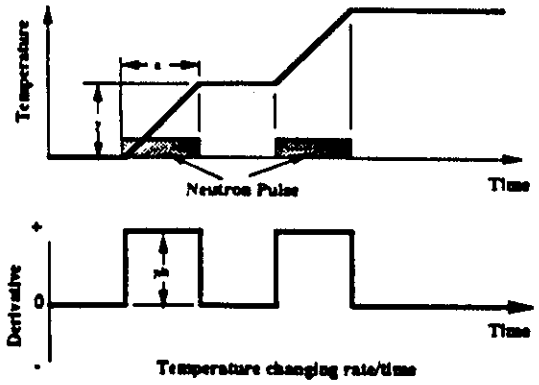

Fig. 1 Conceptual drawing of the temperature rise observation.

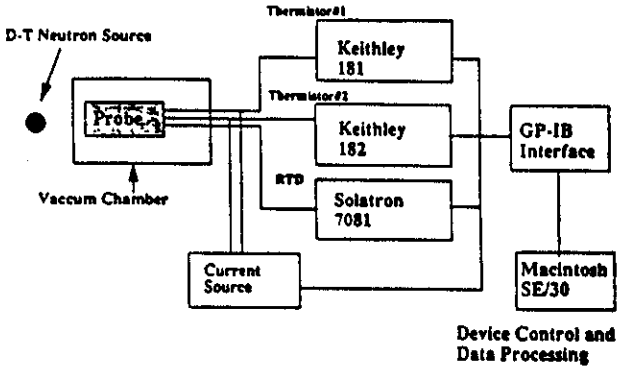

Fig. 2 Block diagram of direct nuclear heating measurement with micro-calorimeter.

observation of temperature change. The differentiation makes it possible to have a S/N in the range of a factor of ten or more. For this purpose, we used the most sensitive low voltage voltmeter currently available, Keithly Model-182 with $8_{1/2}$ digit effective sensitivity along with a former model Keithly 181 and a precision voltmeter, Solatron 7081 both with $7_{1/2}$ digit effective sensitivity.

2.2 Experimental configuration

A block diagram of the present system for the nuclear heating is shown in Fig. 2. The D-T neutron source using a rotating target at FNS[9] was used to bombard the probe materials which was put in a vacuum chamber. Distances of the probes from the neutron source position ranged from 3.6 to 4.0 mm. The schematic configuration of the microcalorimeter is given in Fig. 3. The vacuum chamber was covered with a layer of polystyrene foam to insulate ambient change of room temperature. This configuration cut the thermal conduction and convection from the surrounding area. Two types of thermal sensors were used; two thermistors (TM with 10 kΩ) placed at the front and rear surface of the probe, and a platinum resistance thermo-detector (RTD with 100 Ω) attached on the side. The sensors were connected by a thin wires with voltmeters. All metal probes had a cylindrical dimension with about 20 mm-dia. and 20 mm- hight, the axis of which aligned to the direction from the neutron source. The probe was supported by a thin carbon papers in order to reduce thermal conduction. The four pole measurement was performed for RTD with less resistance to mitigate the effect of resistance of connecting wires. The sensors were contacted directly on the probe materials with use of organic tape. The coefficient of the sensors for the temperature change were 2.04×10^{-3} Ω/K and 2.53 Ω/K for TM and RTD, respectively. The temperature rise of 10^{-5} K/sec corresponded to voltage change of 10^{-7} volts when 1 mA and 10 μA currents applied on 100 Ω and 10 kΩ,respectively, resulting in the last one or two digits change of the nano-voltmeters used (Keithly 181 and 182, and Solatron 7081). This means that stability of the system for the ambient temperature change is very crucial to get meaningful signal.

In order to examine the effect of scattered neutrons from surrounding materials on the nuclear heating, an assembly of Li_2CO_3 was constructed to cover the microcalorimeter. The thickness of Li_2CO_3 layer was 200 mm. The front part of assembly was open to make the distance of probe from the source equal as the measurement

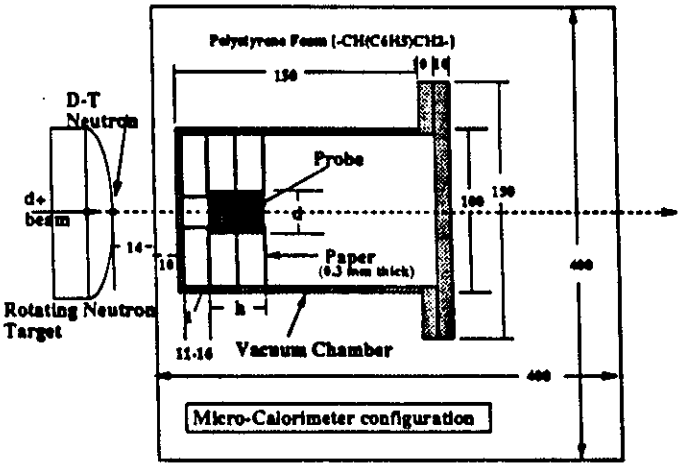

Fig. 3 Cross sectional view of microcalorimeter and experimental configuration.

without assembly. The graphite probe was tested with this Li_2CO_3 assembly.

2.3 Probe Materials

Properties (specific heat, thermal conductivity, density) and dimensions for the probe materials used are shown in Table 1. Only lithium carbonate (Li_2CO_3) has a cubic shape with 250 mm^3. The specific heat data[17] are used to arrive at the final temperature rise. Note that there were large discrepancies in the specific heat data among different literatures as shown in Table 1. This would be a large factor of uncertainty in the experimental analysis.

2.4 Neutron source and bombardment of probe

The D-T neutrons were generated by bombarding a tritiated metal target with deuteron beam of 350 kV and 20 mA. The absolute neutron yield was monitored by a ^{232}Th fission chamber calibrated by the associated α counting method[19]. The calorimeter was irradiated with neutrons spacing 3 to 5 min. Before irradiation, we had to wait to stabilize thermal probe system. Sometime, pre-heating of probe was required to facilitate the procedure. Constant current was applied to the resistance thermal sensors throughout the irradiation to detect the signal during the

Table 1 Material properties and dimensions of probes

Materials	Specific Heat* (J/g/K)		Conductance (W/m/K)	Density (g/cm^3)	Dimension (mm)
C+	0.712	(0.540)[c]	160	2.25	21φ x 20
Ti	0.527	(0.528)	22	4.51	21φ x 20
Ni	0.444	(0.440)	91	8.90	21φ x 20
Zn	0.388	(0.381)	119	7.133	21φ x 19
Zr	0.284	(0.301)	22	6.489	21φ x 18
Mo	0.248	(0.255)	135	10.22	21φ x 20
Sn	0.218	(0.226)	67	7.29	26φ x 20
Pb	0.128	(0.130)	35	11.34	19φ x 20
W	0.133	(0.134)	170	19.24	21φ x 20
Nb	0.256	(0.272)	51	8.57	21φ x 20
Li_2CO_3	0.879	(-----)	< 1	1.82	50 x 50 x 50

a) Value at 300°K, b) Graphite,
c) Values in parentheses were taken from Ref-18)

irradiation. Thin niobium foils were placed in front and back sides of the probe to measure the exact neutron flux during the irradiation. The location of probe was deduced from D-T neutron source strength obtained by the fission chamber and the neutron flux derived by using the reaction rate of $^{93}Nb(n,2n)^{92m}Nb$ assuming cross section of 455 mb at 14.8 MeV.

III. EXPERIMENTAL RESULTS

3.1 Temperature change rate reduction

An example of data on graphite measured by RTD is shown in Fig. 4 to illustrate the procedure for data processing. The experimental data of resistance changes were processed to derive temperature rises corresponding to nuclear heating due to the neutron irradiation. The net change of resistance R was given as,

$$R \pm \delta R = Ave(R_s) - \frac{1}{2}(Ave(R_{B_i}) + Ave(R_{B_{i+1}})) \pm (Ste(R_s) + Ste(R_{B_i}) + Ste(R_{B_{i+1}})),$$

where,
R_s : Resistance at a region of signal,
R_B : Resistance at a region of background,
$Ave(R_S)$:Averaged mean value for R_S,
$Ave(R_B)$:Averaged mean value for R_B,
$Ste(R_S)$:Standard error for R_S,
$Ste(R_B)$:Standard error for R_B.

The temperature rise was obtained by multiplying the conversion coefficient C_α for each thermal sensor, TM(2.04 x 10^{-3} K/Ω) and RTD (2.53 K/Ω).

The temperature rise per source neutron, T, is given as,

$$T = C_\alpha \cdot R/t/Y_n \quad [K/source\ neutron],$$

where,
t ; cycle time for data acquisition [s],
Y_n ; Source neutron strength [/s].

The experimental data were given as an average between the front and rear for thermistor and averaging data for all shots. All temperature changing rates measured are summarized in Table 2.

Table 2 Experimental results

Material	Temperature Rise(K /source neutron) TM)[a]	F/R*	RTD	TM/RTD
Graphite	1.087E-16[b]	1.07	1.132E-16	1.04
Ti	3.769E-17	1.29	4.320E-17	1.17
Ni	7.443E-17	1.21	8.456E-17	1.14
Zr	6.291E-17	2.40	7.440E-17	1.43
	8.885E-17[c]			
	3.697E-17[d]			
Nb	5.168E-17	1.27	5.818E-17	1.13
Mo	5.119E-17	1.19	5.757E-17	1.13
Sn	4.362E-17		4.741E-17	
Pb	8.681E-17	1.12	9.178E-17	1.06
W	9.405E-17	1.06	9.543E-17	1.02
Li_2CO_3	1.132E-16[e]	------		-----
	2.728E-17[f]			
	4.280E-17++, 4.567E-17**			
	7.014E-17***			
Graphite (with Assembly)	8.248E-17	1.10	9.598E-17	1.16

*; ratio between data at front and rear for TM,
**; value at middle of probe,
***; mean value of front and rear data of thermistors,
++; data at the end of irradiation,
a) Averaged value of data at front and rear,
b) reads as 1.2137 x 10^{-16},
c) Front of Zr,
d) Rear of Zr,
e) Front of Li_2CO_3,
f) Rear of Li_2CO_3.

3.2 Graphical representation of nuclear heating signals

Figure 5.1 shows the data for the Mo probe measured by TM. The data for the Sn probe measured by TM and RTD are shown in Figs. 5.2 and 5.3, respectively. Figure 5.4 and gives data for the Li_2CO_3 probe.

Higher value was always found for the data on the front in comparison with the rear data. The ratios of front to rear are also shown in Table 2. In general, material with lower thermal conductivity gives a higher ratio. This reflected the thermal conduction problem in short integration time of 10s (cycle time). Since the probe was exposed in strength D-T neutrons at the close vicinity of neutron source, a steep gradient of nuclear heat deposition along the axis of the probe makes heat flow in the material. In the integration time for ten seconds, equilibrium could not be accomplished, so that slight imbalance was expected. This situation is clearly observed in Fig. 5.1 and 5.2. A fast and larger rise on the front and slow and smaller rise on the rear were detected at the beginning of the neutron shot. The data gradually approached to an identical value at the end of the irradiation. In particular, clear overshoot and undershoot of

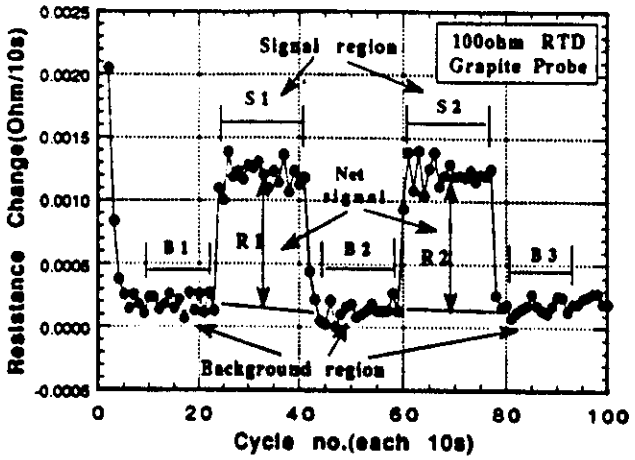

Fig. 4 Scheme for processing of experimental data reduction.

resistance change on the front as shown in Fig. 5.2 indicated thermal conduction phenomena at the boundary for the pulsed heating source. The previous experiment adopting 20 to 30 sec for the integration time mitigated the imbalance in temperature equilibrium at both the ends of probe. Contrary to TM, RTD attached parallelly to the axis on the side didn't show any visible anomalous change in the resistance changing rate during the irradiation as shown in Fig. 5.3. Especially in the material probe of Li_2CO_3 with low thermal conductivity, there was a recognition of more enhanced time dependency in the heat flow in the probe materials during irradiation as shown in Fig. 5.4. This figure shows explicitly the process of equilibrium of temperature according to the gradient of heat deposition rate distribution.

There were slight differences between temperature rises measured by TM and RTD. The data of RTD gave systematically larger value than averaged data of TM by 5 to 10 %, depending on the materials. The TM data at front were identical within experimental errors to the RTD data. The ratios of RTD to TM are also given in Table 2.

Note that as shown in Figs. 5.1, 5.2 and 5.4, the data measured by Keithly 182 with better sensitivity voltmeter offer a factor of 3 less scattered profiles in comparison with

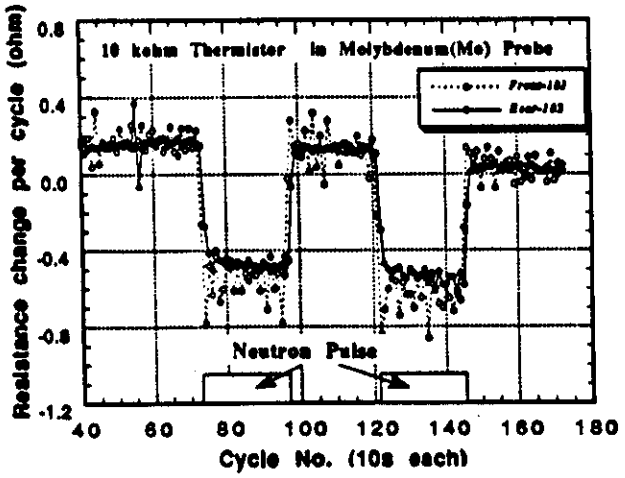

Fig. 5.1 Resistance changes in Mo due to D-T neutron irradiation measured by TMs.

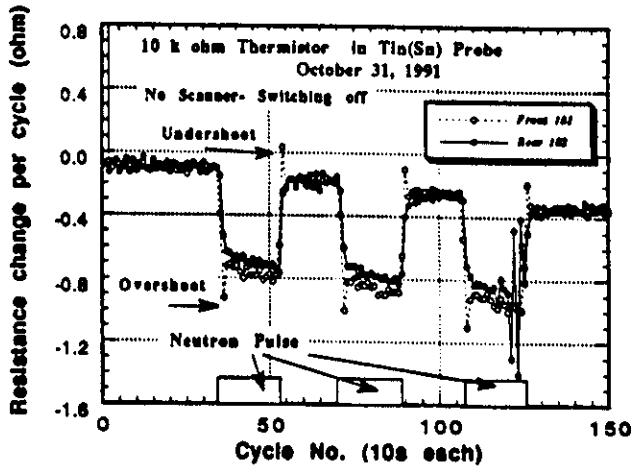

Fig. 5.2 Resistance changes in Sn due to D-T neutron irradiation measured by TM.

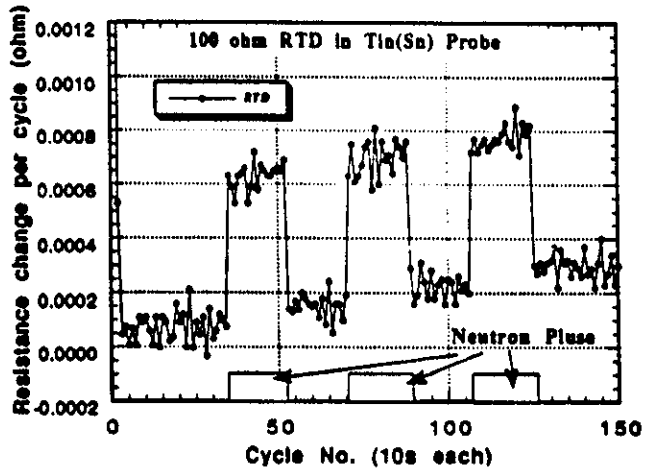

Fig. 5.3 Resistance change in Sn due to D-T neutron irradiation measured by RTD.

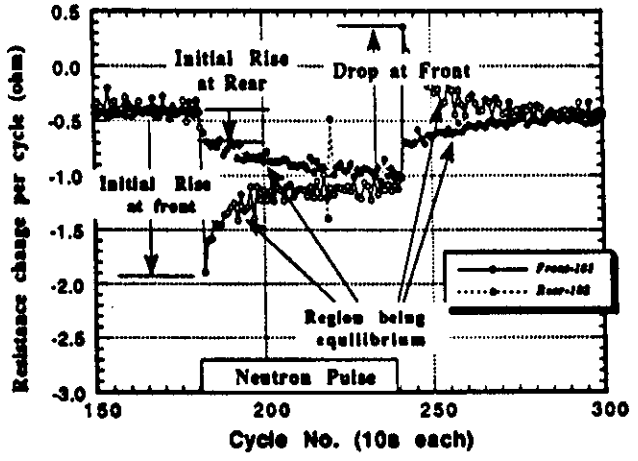

Fig. 5.4 Resistance changes in Li_2CO_3 due to D-T neutron irradiation measured by TM.

the data measured by Keithly-181, the former model of Keithly-182. In addition, the constant current apply without switching made the system more stable. These improvements made cycle time shorter by a factor of 2 to 3 than the previous experiments[1,2]. As a results, overall experimental errors could be reduced less than 10 %, while errors in the previous measurements were more than 20 %.

3.3 Experimental errors

The self-heating driven by the joule heat in resistance of sensor gave constant heating load which contributed constant change of the temperature. If the weight of sensor was assumed to be 10^{-3}/g, the heat generation was equivalent to 10^{-3} W/g, resulting in much higher rate than that in nuclear heating process ranging from 10^{-4} to 10^{-5} W/g.

The other factor to be considered was the contribution to the temperature change from heat conduction even though it was small and slow. Even in the circumstance with good air conditioning, the change of 10^{-2} K is possible. This change makes a steep gradient in the temperature between the probe and circumstance in comparison with the temperature change due to the nuclear heating. The fluctuation of the drift line was attributable to electrical noise (it may be some timing effect) and slow change of the ambient temperature change in the room.

As mentioned, the distance of probe from the neutron source was determined by using neutron source strength and reaction rate of Nb foil activation. A change of 1 mm in the distance of 37 mm made a maximum change of 4 % in the heating rate as long as the calculation of JENDL-3 was concerned.

The experimental errors are tabulated in Table 3. In the present data processing, we assumed adiabatic thermal insulation; no thermal convection, conduction and radiation between probe and environment.

Table 3 Uncertainties of experimental data

Item	Estimated error (%)
1. Fluctuation of drift curve in derivatives (Standard error)	3 - 7
2. Background of drift curve	2 - 3
3. Positioning	3 - 5 (Systematic)
4. Source neutron strength	2.5 (Systematic)
Total	5.3 - 9.4

IV. ANALYSIS

The neutron and gamma-ray transport calculation was carried out by using the two dimensional code DOT3.5[20] and the three-dimensional code MCNP[21] with nuclear data libraries: FUSION-J3[22] based on JENDL-3[23] for DOT3.5 and RMCCS[20] for MCNP. Both calculations modeled the experimental system as precisely as possible, including the rotating neutron target structure, microcalorimetric system and the target room. In the DOT3.5 calculation, P_5S_{16} approximation was used for R-Z model and the first collision source was calculated by the GRTUNCL code. A KERMA factors of neutron and γ-ray for DOT3.5 calculations were generated from the JENDL-3 by using NJOY processing code[24] and from DLC-99[25] by energy balanced method,[26] respectively. Heating number of four libraries available[21] with MCNP, i.e., RMCCS, ENDF5T, ENDL85[27] and BMCCS based on ENDF/B-IV were used for the MCNP calculations. The calculated heating rate in each material was converted to the temperature rise in the unit of K/source neutron to be compared with the measurement. In this analysis, we didn't treat time dependent thermal conduction during finite irradiation time. The value to be compared with experiment was derived averaging data over entire volume of probe except for Li_2CO_3 which has a considerably low thermal conduction so that the time dependent profile should be taken into account.

Comparison of measurement and calculation was performed in a dimension of temperature (K). Since the calculation provided nuclear heating in J/g/source, the specific heat (J/g/K) was used to arrive at the temperature rise in K.

V. DISCUSSION

Figure 6 gives calculated fractions of neutron and γ-ray along with total heat deposition rate in an order of Z number. There are general trends in the ratio between neutron and γ-ray contributions as well as the heat deposition rate itself as a function of Z number: (1) Lower Z materials have large neutron contribution, while higher Z materials have large sensitivity to γ-rays. (2) Heat deposition rate decreases with Z number. This calculation was based on JENDL-3.

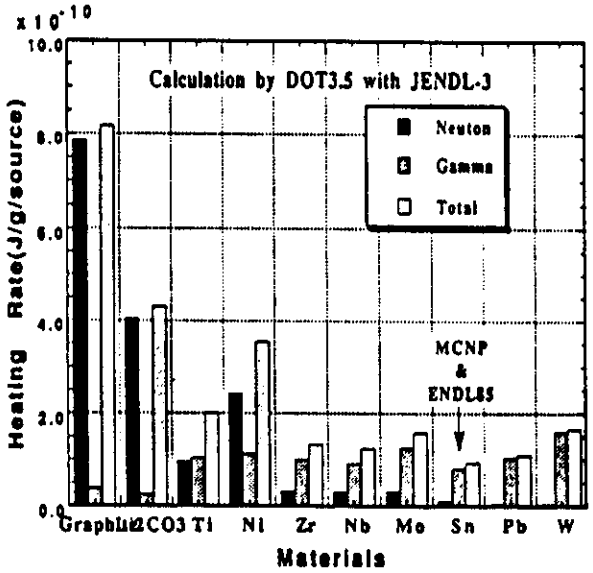

Fig. 6 The fractional contribution of neutron and γ-ray to the total heating rate calculated by DOT3.5 using JENDL-3 nuclear data library.

Table 4 gives a summary of ratios of calculation to experiment (C/E) corresponding to all KERMA libraries tested here. The experimental values by TM were used for comparison with calculations. It was proved that the RMCCS and ENDF5T were identical as far as the C/E values were concerned here. Material wise discussion is as follows;

Graphite: All calculations overestimated measurements in both cases with and without the Li_2CO_3 assembly. The calculation with JENDL-3 and ENDL85 gave overestimations of experiments by 20 %, while others

Table 4 Summary of C/E values

Material	JENDL	RMCCS	ENDF5T	ENDL85	MBCCS
C	1.19	1.34	1.34	1.22	1.38
C*	1.17	1.34	1.34	1.22	1.39
Ti	1.05	1.06	1.06	1.04	0.88
Ni	1.11	1.39	1.39	1.21	1.87
Zr	0.82	2.09	2.09	0.40	0.31
Nb	1.00	1.04	1.04	0.94	0.79
Mo	1.23	0.84	0.84	0.96	0.84
Sn	-----	0.98	-----	0.98	3.51
Pb	1.14	1.44	1.44	1.00	1.46
W	1.32	1.18	-----	1.17	-----
Li_2CO_3	1.00	0.98	0.99	-----	1.00
Front	1.41	1.25			
Middle	1.16	1.37			
Rear	1.30	1.06			

* with Li_2CO_3 assembly

overestimated them by 30 to 40 %. Considering experimental errors ranged within ± 5 %, these discrepancies seemed large regarding that graphite is most essential materials, in particular, one of reference materials for the heating consideration. One possible reason for the overestimation could be attributable to the data of specific heat for graphite. As described before, the specific heat data is not well defined because it differs sample by sample. The graphite material used was not well specified, possible with less density, so that actual specific heat data could be lower than that used in the calculation.

Titanium: All calculation except MBCCS gave good agreements with measurement; C/Es were 1.04 to 1.06; C/E of MBCCS was 0.88.

Nickel: For nickel, all calculation gave similar C/E as for graphite. The calculation based on JENDL-3 gave the best agreement with experiment (C/E=1.11) among all calculations. An exceptionally large overestimation was found in MBCCS, giving C/E of 1.87.

Zirconium: The C/E values exhibited a very scattered nature. The most preferable C/E was found in JENDL-3, whereas the others overestimated and underestimated by more than a factor of 2. The MBCCS gave the worst C/E of 0.31. This was the case with the most discrepant results in different libraries. Since the experimental probe was made by stacking a thin discs, less thermal conductance than that of a single material should be taken into account for the reduction of experimental data. Not only the library data, but also experimental data should be re-examined in the future.

Niobium: All calculations, except one by MBCCS gave satisfactory results in terms of C/E values, as shown in titanium case. The calculation with MBCCS underestimated experiment by more than 25 %.

Molybdenum: Only the calculation with JENDL-3 overestimated experiment by 23 %, while the others underestimated it 4 to 20 %. The calculation with ENDL-85 gave the best agreement with experiment. These C/E trends were similar to those in previous experimental analysis.[6]

Tin: The JENDL-3 and ENDF5T didn't include data of tin. Though the calculations with RMCCS and ENDL-85 gave good agreements with experiment, the calculation with MBCCS overestimated it by a factor of 3.5. The neutron contributions were 13 % in both the RMCCS and ENDL-85, and 76 % in the BMCCS. From a systematics of mass dependency as shown in Fig. 6, the 76 % the neutron contribution appeared in the MBCCS calculation seemed extremely high. This would be the reason for large overestimation.

Lead: Though the calculations with JENDL-3 and ENDL-85 gave reasonable agreements with experiment, calculations with RMCCS, ENDF5T and BMCCS overestimated it by 44 to 46 %. These overestimations were attributable to the large neutron contributions of about 34 % by the same consideration of systematic trend shown in Fig. 6 as seen in tin case.

Tungsten: No heating number data was found in ENDF5T and MBCCS. The calculations with JENDL-3, RMCCS and ENDL-85 overestimated experiment by 32, 18 and 17 %, respectively. This range of overestimation was consistent with that in the previous experimental analysis.[5,6]

Lithium Carbonate: The C/E values close to 1.0 for all calculations indicated the adequacy of data for heating numbers, i.e. KERMA factors as long as the averaged value over the entire volume of probe. As shown in Fig. 5. 4, however, a more precise analysis should be required by taking the time dependency of temperature change during irradiation:

The Li_2CO_3 probe made by sintering the Li_2CO_3 powder was the effectively lowest Z-material among materials tested. As naturally understood, the thermal conductivity of the ceramic was extremely low in comparison with ordinary metal. Even though such a low conductivity, a duration for ten seconds was not enough to neglect the heat flow, so that the equilibrium in the heating rate was observed after a few sampling of the data.

Tungsten demonstrated a capability for the γ-sensitive probe its large and small sensitivities to neutron and γ-ray, respectively. While the material itself produces a lot of γ-rays. In this regard, lead seems more attractive, even though low melting point limits the temperature to be measured. Graphite is the promising neutron probe. The combination of the both materials with less interaction each other may be the excellent neuclear heating probe system.

VI. CONCLUSION

Nuclear heat deposition rate in ten materials of lithium carbonate, graphite, titanium, nickel, zirconium, niobium, molybdenum, tin, lead and Tungsten, subjected in the 14 MeV neutron flux were measured and compared with the calculations with currently available nuclear data relevant. The improvement on the accuracy in the measuring system gave excellent S/N in the measurement of the temperature rise during the bombardment with 14 MeV. Range of overall errors fell within 10 %. The calculation based on JENDL-3 and ENDL-85 gave better results than calculations with the other libraries. However, still, the large uncertainty was found in the data for the specific heat, which differ reference by reference. The best solution for this is to measure the specific heat for the particular materials to be measured. The other uncertainty was in the time dependency in the thermal conduction in the probe itself, during irradiations. In order to solve this problem, the sampling time should be shorten to be range in which the thermal conduction is negligible. Finally, we would declare that experimental technique has been established. The results encouraged us to proceed in the measurement in the large system with better simulation of

D-T neutron environment, data in which feedback more direct test of the codes and data.

ACKNOWLEDGEMENTS

The authors would like to express their sincere thanks to Messers. J. Kusano, C. Kutsukake, S. Tanaka and Y. Abe for operation of FNS accelerator in the particular experimental request. Dr. T. Nakamura was grateful for his valuable advice and encouragement for the experimental program in the earlier stage. The work of US contribution was supported by USDOE.

REFERENCES

1. M. A. ABDOU, C. W. MAYNERD and R. Q. WRIGHT, "MACK: A Computer Program to Calculate Neutron Energy Release Parameters (Fluence-to-Kerma Factor) and Multigroup Reaction Cross Sections from Nuclear Data in ENDF Format," ORNL-TM-3994 (Jul. 1973).
2. M. A. ABDOU and C. W. MAYNARD, "Calculation Method for Nuclear Heating -Part I: Theoretical and Computational Algorithms," Nucl. Sci. Engrg. 56 (1975) 360.
3. M. A. ABDOU and C. W. MAYNARD, "Calculation Methods for Nuclear Heating- Part II: Applications to Fusion Reactor Blanket and Shields," *Nucl. Sci. Engrg.* 56 (1975) 381.
4. Y. FARAWILA, Y. GOHAR and C. W. MAYNARD, "KAOS/LIB-V: A Library of Nuclear Response Functions Generated by KAOS-V Code from ENDF/B-V and Other Data Files," ANL/FPP/TM-241 (1989).
5. K. MAKI, H. KAWASAKI, K. KOSAKO and Y. SEKI, "Nuclear Heating Constant KERMA Library," JAERI-M 91-073 (1991). (in Japanese)
6. M. KAWAI, S. IIJIMA, T. ARUGA, et al., "Reviw of the Research and Application of KERMA Factor and DPA Cross Section," JAERI-M 91-043 (1991). (in Japanese)
7. Y. IKEDA, C. KONNO, K. KOSAKO and D. P. KUHN, "Direct Measurement of Temperature Rise in Structural Materials Due to Nuclear Heating by 14 MeV Neutrons," JAERI-M 89-128 (1989) pp. 153-154.
8. D. P. KUHN, Y. IKEDA, C. KONNO and W. VATH, "A Calorimetric Measurement of the Nuclear Heating Effect in Steel and Graphite Caused by 14 MeV Neutrons," KFK report, to be published.
9. T. NAKAMURA, H. MAEKAWA, J. KUSANO, Y. OYAMA, Y. IKEDA, C. KUTSUKAKE, S. TANAKA and Shu. TANAKA, "Present Status of the Fusion Neutron Source(FNS)," *Proc. 4th Symp. on Accelerator Sci. Technol.*, RIKEN, Saitama, 24 - 26 November (1982) 155-156.
10. A. KUMAR, Y. IKEDA and C. KONNO, et al., "Experimental Measurements and Analysis of Nuclear Heat Deposition Rates in Simulated D-T Neutron Environment: JAERI/ USDOE Collaborative Program on Fusion Neutronics Experiments," *Fusion Technol.* Vol. 19, 3, Part 2B (1991) pp 1979 -1988.
11. A. KUMAR, Y. IKEDA, C. KONNO, et al., "Direct Nuclear Heating Measurement in Fusion Neutron Environment and Analysis," *Fusion Eng. and Design.* 18 (1991) pp 397 - 405.
12. S. R. DOMEN, "Advances in Calorimetry for Radiation Dosimetry," pp. 245-320, in "The Dosimetry of Ionization," Vol. II, edited by K. R. Kase, B. E. Biangrad and F. H. Attix, Academic Press, Inc., Orlando (1987).
13. S. R. GUNN, "Radiocalorimetric Calorimetry: A Review, "*Nucl. Instrum. Methods*, 29, 1 (1964); also other two later reviews with identical titles in *Nucl. Instrum. Methods*, 85, 285 (1970) and *Nucl. Instrum. Methods*, 135, 251 (1976).
14. S. R. DOMEN and P. J. LAMPERTI, "A Heat-loss-compensated Calorimeter:Theory, Design and Performance," *J. Res. Nat. Bur. Stand.* (U. S.) (Phys. and Chem.), 78A(5): 595 (1974).
15. J. S. LAUGHLIN and S. GENNA, "Calorimetry," pp. 380-441, in "Radiation Dosimetry", Vol. II, edited by F. H. Attix and W. C. Roesch, Academic Press Inc., New York (1966).
16. J. A. MASON, A. N. ASFAR and P. J. GRANT,"Improved Microcalorimetry for Radiation Absorbed Dose Measurement," Proc. 5th ASTM Euratom Symp. on Reactor Dosimetry, Vol. 1, (1984) pp. 415-423.
17. Y. S. TOULOUKIAN and E. H. BUYCO, Specific Heat: Metallic elements and alloys, Vol. 4 of Series on Thermophysical Properties of Matter (IFI/Plenum, New York, 1970); see also, by same authors, " Specific Heat: nonmetallic solids, Vol. 5 of the series, (IFI/Plenum, New York, 1970).
18. "JSME Data Book: Heat Transfer," 3rd Edition, Japanese Society of Mechanical Engineering, (1975).
19. H. MAEKAWA, Y. IKEDA, Y. OYAMA, S. YAMAGUCHI and T. NAKAMURA, "Neutron Yield Monitors for the Fusion Neutronics Source (FNS), JAERI-M 83-219 (1983).
20. W. A. RHOADES and F. R. MYNATT, "The DOT III Two-Dimensional Discrete Ordinates Transport Code," ORNL/TM-4280 (1979).
21. J. F. BREISMEISTER, ed., "MCNP-A General Monte Carlo Code for Neutron and Photo Transport: Version 3A," Report No. LA-7396-M, Rev. 2 (Sep. 1988), along with MCNP3B newsletter dated Jul. 18, 1988, Los Alamos National Laboratory.
22. K. MAKI, K. KOSAKO, Y. SEKI and H. KAWASAKI, "Nuclear Group Constant Set FUSION-J3 for Fusion Reactor Nuclear Calculations Based on JENDL-3," JAERI-M 91-072 (1991).
23. K. SHIBATA, T. NAKAGAWA, T. ASAMI, et al., "Japanese Evaluated Nuclear Data Library, Version-3," JAERI-1319 (1990).
24. R. E. MACFARLANE, D. W. MUIR and R. M. BOICOURT,"The NJOY Nuclear Data Processing System, Volume II: The NJOY, RECONR, BROADR, HEATR and THERMR Modules," LA-9303-M, Vol. II (ENDF-324) (1982).
25. R. J. HOWERTON, "Calculated Neutron Kerma Factors based on the LLNL ENDL data file," UCRL 50400 Vol 27 (Jan. 1986).
26. R. W. ROUSSIN, J. R. KNIGHT, J. H. HUBBELL and R. J. HOWERTON, "Description of DLC-99/ HUGO Package of Photon Interaction Data in ENDF/B-V Format," ORNL/RSIC-46 (ENDF-335) (1983).
27. R. MACFARLANE, "Energy Balance of ENDF/B-V," Trans. Am. Nucl. Soc. 33 (1979)681.